Cooperative Maneuver Planning for Mixed Traffic at Unsignalized Intersections Using Probabilistic Predictions

Max Bastian Mertens[1], Johannes Müller[1], and Michael Buchholz[1]

***Abstract*— Intersections are among the scenarios that are most crucial for efficiency and traffic flow on roads. Several approaches to traffic control at intersections exist, each with its own advantages and drawbacks. These days, wireless connections between road users, automated vehicles, and intelligent infrastructure enable new ways of coordinating traffic. However, the gradual deployment of those advanced technologies leads to a heterogeneous mixture of partially automated, connected, and legacy vehicles. Planning and coordinating maneuvers for this mixed traffic is a challenge and subject to current research, as it can achieve significant efficiency improvements in those scenarios. In this paper, we propose a new maneuver planning system for cooperative connected vehicles in mixed traffic at unsignalized intersections, which often occur in urban areas. Our system consists of a probabilistic multi-modal prediction based on a driver model and an efficient optimization algorithm to find the best maneuvers. We present the functionality of our approach and evaluate the impact on traffic efficiency using simulations of two different intersection layouts at various rates of cooperative vehicle penetration.**

I. Introduction

Traffic efficiency is key to urban mobility of the future. Connected automated vehicles (CAVs) can contribute to an improved traffic efficiency with cooperative maneuvers, e.g., at unsignalized intersections. In this case, cooperation means that individual road users accept a small loss of efficiency to achieve an overall improvement of efficiency, i.e., traffic flow. To exploit this potential, many ideas have been proposed so far, as can be seen by the standardization efforts for cooperative communication by the European Telecommunications Standards Institute (ETSI) [1]. However, mixed traffic of CAVs and unconnected (legacy) vehicles still poses a big challenge to existing cooperation schemes. Some approaches combine CAVs and traffic lights [2], however, even modern adaptive traffic light switching [3] uses inflexible plans that block whole lanes and have long switching times. On the other hand, individual coordination of the crossing order has an exponential complexity in the number of road users [4]. Approaches can therefore scale poorly, while a high number of participants is important to reach high efficiency gains.

In this work, we propose a novel centralized maneuver planning scheme for mixed traffic focusing on the individual control of cooperative vehicles at unsignalized intersections.

This work was financially supported by the Federal Ministry for Economic Affairs and Climate Action of Germany within the program "Highly and Fully Automated Driving in Demanding Driving Situations" (project LUKAS, grant number 19A20004F).

[1]The authors are with the Institute of Measurement, Control and Microtechnology, Ulm University, D-89081 Ulm, Germany. E-mail addresses: {max.mertens, johannes-christian.mueller, michael.buchholz}@uni-ulm.de

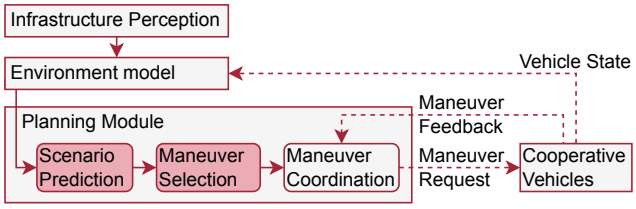

Fig. 1. Cooperative planning context overview. This work focuses on the scenario prediction and maneuver selection modules described in Section II and evaluated in Section III. V2X communication is marked dashed.

In this context, we refer to *maneuvers* as a dynamic intervention enforcing a specific crossing order among cooperative vehicles, possibly deviating from the order implied by static traffic rules, to increase the efficiency of overall traffic. We use the term *efficiency* to refer to a high traffic throughput, i.e., higher velocities and lower waiting times at intersections, defined more concisely in Section II. Our approach considers CAVs as well as connected non-automated vehicles (CVs), collectively referred to as *cooperative vehicles*, as elaborated in Section II-B. The planning system is supposed to run on smart infrastructure located at an intersection. Coordinating conflicting traffic at a narrowing road, at a construction site, or at a highway on-ramp can also be handled by our approach, but are out of scope of this paper.

Figure 1 gives an overview and context of the proposed cooperative planning system. It comprises three steps: First, an environment model obtained from infrastructure sensors and connected vehicles is used for a probabilistic, model-based, multi-modal prediction of the scenario over time. For each predicted scenario outcome, the probability and efficiency are estimated and sorted into a decision tree. Second, we developed an efficient optimization algorithm to select the maneuver resulting in the highest overall expected traffic efficiency. Third, we coordinate the maneuver in a feedback loop with vehicle-to-anything (V2X) communication.

A. Related Work

Several approaches to traffic control at unsignalized intersections have already been proposed. Early works handle the exponential complexity of individual control with heuristics, such as first come, first served [5] or by plain enumeration [4], [6]. More advanced approaches use optimization techniques, such as dynamic programming [7], mixed-integer quadratic programming [8], or tree based search methods [9], [10], to find the most efficient crossing order. The approach in [11], also from our research project, uses reinforcement learning to generate efficient schemes. However all these pro-

posals focus on uniform CAV-only traffic, where a specific order can be easily imposed on the vehicles.

Only few published approaches handle mixed traffic, such as [2], where traffic lights are used to incorporate and control legacy vehicles. However, the route of legacy vehicles still has to be known for their planning system to work. The authors of [12] took a similar approach with traffic lights and handled legacy vehicles with unknown route by reserving all possible trajectories at the intersection. However, they focus on a cooperative vehicle rate of $90\,\%$ and above with the use case of malfunctioning V2X communication in an otherwise homogeneous cooperative-vehicles-only traffic. Connected non-automated vehicles (CVs) are only considered by few approaches, such as [13], [14], where a vehicle-specific traffic light is shown to the driver in an on-board human machine interface (HMI). In contrast, with our approach, we handle any amount of cooperative vehicles, i.e., CAVs and CVs, in mixed traffic and consider legacy vehicles for maneuver feasibility and in the overall traffic efficiency estimation. We show that a noticeable efficiency gain can already be reached at low cooperative vehicle ratios.

The coordination of maneuvers is usually performed by reservations for a certain time, either for the whole intersection [4], for a discrete grid in space and time [5], or for continuous time intervals along the route [15]. However, reserving the whole intersection or discrete parts of it is an approximation due to which some potential efficiency gain can be missed. We proposed a variant of the ETSI Maneuver Coordination Message (MCM) [16], combining the existing approaches and use continuous time interval reservations for the parts of an intersection where lanes cross or merge. We incorporate CVs by reserving larger time intervals, which can be presented to the driver on the on-board HMI. For the simulations in this paper, a more high-level encoding was used as described in Section II-B.1.

B. Contribution

We present a novel approach for cooperative maneuver planning that is able to handle mixed traffic with CAVs, CVs, and legacy vehicles at unsignalized intersections. Our maneuver planning algorithm is based on a new probabilistic, multi-modal prediction with a decision-tree representation. The optimization algorithm scales quadratically with the number of participating vehicles and is therefore computationally more efficient compared to the enumeration of combinations with exponential complexity. Our evaluation based on a microscopic traffic simulation at two different intersection types shows that we achieve significant efficiency gains even for a medium cooperative vehicle penetration rate.

II. Approach

In this section, we formulate the problem and assumptions and present our approach to cooperative maneuver planning.

A. Problem Definition and Assumptions

This paper focuses on traffic control using cooperative maneuvers in a fixed area around an unsignalized intersection. We assume that there is a connected infrastructure providing scene perception and computational resources for the planning system. We consider mixed traffic consisting of cooperative vehicles, i.e., CAVs and CVs, and legacy vehicles. Cooperative vehicles are connected via wireless V2X communication such as ITS-G5 [17] or cellular network. They can be automated or steered by a human driver who receives maneuver requests via a human-machine interface. The maneuver planning can individually control the available cooperative vehicles in the scene as described in Section II-B.1, considering also the behavior of all present legacy vehicles. The aim of the planning system is to generate maneuvers to optimize the overall traffic flow, i.e., to reach higher average velocities and lower waiting times. The quantitative measure used for evaluation is given in Section III-B.

For our approach, the traffic at the considered area has to be completely observed by the infrastructure perception as long as legacy vehicles have to be considered. Road users other than vehicles are currently not considered and may not be present at the scene. For each vehicle V_i ($i \in \{1, \dots, N_\mathrm{V}\}$) in the scene at time t, the position $\boldsymbol{x}_i(t)$ and velocity $v_i(t)$ have to be provided in the environment model. The planned route of legacy vehicles is not known to the planning module if there is no separate turn lane present at the observed intersection. This is handled by assuming that those vehicles could take any of the possible turns and are probably in conflict with all other lanes, just as in [12].

B. System Overview

An overview of the cooperative planning system is given in Fig. 1. Infrastructure must provide perception of all road users within the considered area. Connected vehicles can additionally provide more accurate vehicle states and their planned routes. The road user information is combined into a comprehensive environment model, which provides the position and velocity of each vehicle in the scene. The planning module frequently analyzes the environment model. For a given scenario, multiple possible outcomes are predicted, which may result from different driver behavior and the possible maneuvers. Each prediction is evaluated to estimate the impact of the various maneuvers on the traffic efficiency. The best maneuver is carried out by a coordinating module and the involved cooperative vehicles.

1) Maneuver Encoding and Coordination: The coordination of maneuvers is not the focus of this paper, so only the key points are summarized here. Maneuvers are performed by assigning priorities between cooperative vehicles, possibly deviating from their default precedence, i.e., right of way. As a result, a specific crossing order among them can be enforced, allowing an increase of efficiency in overall traffic. Only cooperative vehicles within the range of the infrastructure perception, but far enough to the intersection to react, are considered as maneuver participants.

Drivers in legacy vehicles assume other road users to follow the default precedence rules. Therefore, whenever a legacy vehicle might be affected by a cooperative vehicle priority reassignment, no maneuver is planned to guarantee safety. After each planning cycle, it is checked again if the

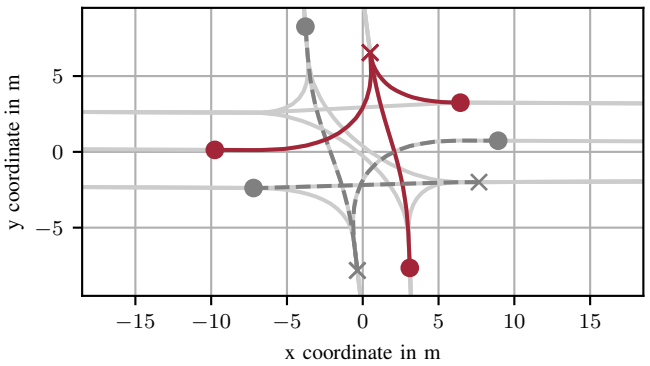

Fig. 2. Intersection at Bendplatz (Aachen, Germany) with a horizontal main road that has separate left turn lanes. This figure shows all lanes (light gray) and two exemplary conflict zones at crossing (dark gray, dashed) and merging (red) lanes, including their start (circle) and end (cross) points.

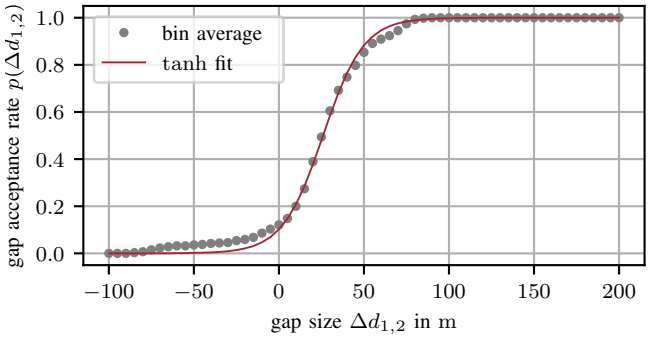

Fig. 3. Gap acceptance between two vehicles approaching an intersection as observed in the SUMO simulator. $p(\Delta d_{1,2}) = p(d_2 - d_1)$ is the probability of vehicle V_1 on a side road taking precedence over V_2 on the main road. The figure shows acceptance rates averaged over bins and a tanh model.

resulting maneuvers are still valid and can be carried out, otherwise they are discarded. Therefore, using our planning scheme, no unsafe maneuver is coordinated and maneuvers only have an effect on the efficiency, not on the safety of a situation. Maneuvers chosen in one planning cycle are pursued as long as at least two of the relevant vehicles still approach the intersection, so already planned maneuvers are never modified.

2) Consolidating CAVs and CVs: Maneuvers are planned to be encoded in our MCM variant [16], where parts of the intersections are reserved for continuous time intervals. For the evaluations in this paper, however, a more high-level encoding is used and the precedence priorities are directly passed on to the simulation framework. We therefore do not distinguish between CAVs and CVs and collectively refer to them as cooperative vehicles.

3) Real-time constraints and suboptimality: The planning system is run in a continuous loop as frequently as possible. To only pursue maneuvers that are based on an up to date environment model, we restrict the planning cycle to a rate of at least 1 Hz. After a timeout of 1 s, the planning is aborted and no new maneuver is planned in this cycle. To reach this real-time requirement, for a high number of vehicles in the scene, the system might have to resort to approximative algorithms and yield a suboptimal solution. With the encoding and coordination scheme as described in Section II-B.1, by design, only safe maneuvers are performed. Therefore, suboptimality in the maneuver planning is uncritical and just means not finding the highest possible traffic efficiency.

C. Scene Representation and Preprocessing

A representation of the road layout is imported from a map source such as OpenStreetMap and its structure is preprocessed. Areas where two or more lanes cross or merge are marked as *conflict zones* Z_k ($k \in \{1, \ldots, N_\mathrm{Z}\}$). An example intersection is shown in Fig. 2. Conflict zones start where a vehicle has to stop to yield. Intersections may contain multiple conflict zones, and the zones can be overlapping or disjoint. In the prediction described in Section II-D, it is assumed that, at each point in time, vehicles from only one direction may drive on a conflict zone. This representation is easily adapted to arbitrary intersection layouts and other scenarios such as a shared lane at a narrowing road.

D. Scenario Prediction

A traffic scenario received from the environment model is predicted into the future to evaluate the advantage of possible maneuvers. A prediction time horizon of $T_\mathrm{hor} = 6\,\mathrm{s}$ was empirically chosen to allow vehicles close to an intersection to completely cross. The prediction uses a vehicle behavior model with a similar structure as the Intelligent Driver Model [18], considering preceding vehicles but also speed limits, maximum lateral acceleration in curves, and blocked conflict zones. The model calculates the vehicle accelerations in each prediction step and allows for a computationally efficient discrete integration with a time step of $\Delta t = 0.5\,\mathrm{s}$. As only vehicles from one direction are allowed in a conflict zone at the same time, the occupancy of those areas is predicted with a time-continuous reservation scheme.

Legacy vehicles or cooperative vehicles currently not in a coordinated maneuver can behave in various ways within the applicable traffic rules. More impatient drivers accelerate faster and take smaller gaps. The order in which vehicles cross an intersection is therefore unknown. To get an expected value of the maneuver efficiencies, multiple possible predictions of the scenario are made and their probability and efficiency is estimated. For each scenario $\mathcal{S}$ starting at time t, the position and velocity $\boldsymbol{x}_{\mathcal{S},i}(\tau), v_{\mathcal{S},i}(\tau)$ of each vehicle V_i are predicted on the time horizon $\tau \in [t, t + T_\mathrm{hor}]$.

1) Probability estimation: Whenever two or more vehicles from different lanes want to drive on the same conflict zone as defined in Section II-C, a decision must be made. Traffic rules specify the vehicle priority depending on their originating lane or turn direction, where low-priority vehicles can use gaps in prioritized traffic. The probability of a low-priority vehicle taking a gap in the priority lane traffic depends on the gap size [19]. The function $p_{\mathcal{S},\mathrm{Z}}(i, j, \tau)$ denotes the *precedence probability*, i.e., the probability that vehicle V_i takes precedence before V_j at a conflict zone Z

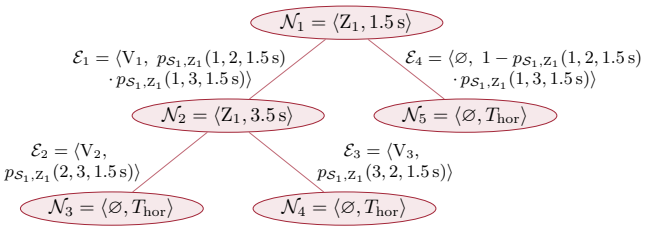

Fig. 4. Exemplary decision tree at $t = 0$ where vehicles $\mathrm{V}_1, \mathrm{V}_2, \mathrm{V}_3$ approach the conflict zone Z_1. Edge $\mathcal{E}_4$ is not explored further, so it directly ends with a leaf node without any further intermediate nodes. Decision trees in the evaluation scenarios have a much higher number of nodes and edges.

at time τ in the predicted scenario $\mathcal{S}$. It is modeled as a sigmoid function

$$p_{\mathcal{S},\mathrm{Z}}(i,j,\tau) \coloneqq \begin{cases} p\left(\Delta d_{i,j}(\tau)\right), & \text{if } \mathrm{V}_i \text{ has to yield} \\ 1 - p\left(\Delta d_{j,i}(\tau)\right), & \text{if } \mathrm{V}_j \text{ has to yield} \end{cases} \tag{1a}$$

$$\text{with } \Delta d_{i,j}(\tau) = d_j(\tau) - d_i(\tau) \tag{1b}$$

$$\text{and } p(\Delta d) = \frac{1}{2}\left(\tanh \frac{\Delta d - a}{b} + 1\right), \tag{1c}$$

where d_i, d_j are the respective distances of $\mathrm{V}_i, \mathrm{V}_j$ to the conflict zone center on their lane. $\Delta d_{i,j}(\tau) = d_j - d_i$ is the virtual gap size of V_i to V_j as used in [19]. The precedence probability is symmetrical, i.e.,

$$p_{\mathcal{S},\mathrm{Z}}(i,j,\tau) = 1 - p_{\mathcal{S},\mathrm{Z}}(j,i,\tau). \tag{2}$$

The gap acceptance $p(\Delta d)$ was parametrized by analyzing a $30\,\mathrm{min}$ simulation of an intersection in the SUMO microscopic simulator [20] with vehicles approaching from $d \leq 250\,\mathrm{m}$ and averaging the gap acceptance rate over gap size bins of $20\,\mathrm{m}$ width, see Fig. 3. The $\tanh$ sigmoid is centered at $a = 26\,\mathrm{m}$ and horizontally scaled by $b = 24\,\mathrm{m}$.

When more than two vehicles approach a conflict zone, the probability of a vehicle taking precedence is the product of all precedence probabilities of this vehicle against the others, see Fig. 4 for an example. Also, the precedence probability between vehicles can vary for every predicted scenario.

2) Efficiency measure: The cooperative planning aims to improve the overall traffic flow and efficiency by increasing the average velocity and reducing the average waiting time. It is therefore desirable for vehicles to reach their speed limit, which is given by traffic rules and curvature. As a quantitative measure for a predicted scenario, we define the efficiency e as the integrated ratio of the velocity to the speed limit over all vehicles:

$$e(\mathcal{S}) \coloneqq \sum_{i=1}^{N_\mathrm{V}} \int_t^{t+T_\mathrm{hor}} w_i \frac{v_{\mathcal{S},i}(\tau)}{v_{\max}(\boldsymbol{x}_{\mathcal{S},i}(\tau))}\,\mathrm{d}\tau, \tag{3}$$

where $v_{\max}(\boldsymbol{x})$ denotes the speed limit at vehicle position $\boldsymbol{x}$, given by traffic rules and curvature. The constant factors w_i can be used to give vehicles an individual weight, e.g., to prioritize public transport, but is set to 1 in all simulations in this paper.

3) Decision Tree Composition: For each potential conflict between two or more vehicles approaching the same conflict zone, a decision has to be taken. The decisions of all predicted scenarios with the respective decision probabilities and scenario efficiencies are represented in a chronologically sorted decision tree. An example tree is shown in Fig. 4. Tree nodes represent a tuple $\mathcal{N} = \langle Z, \tau \rangle$ that describes *where* and *when*, i.e., at which conflict zone $Z \in \{\mathrm{Z}_1, \ldots, \mathrm{Z}_{N_\mathrm{Z}}\}$ and at which time τ, a decision is made. Edges represent a tuple $\mathcal{E} = \langle V, p_\mathcal{E} \rangle$ describing *which* decision is made, i.e., which vehicle $V \in \{\mathrm{V}_1, \ldots, \mathrm{V}_{N_\mathrm{V}}, \varnothing\}$ reserves the conflict zone, and the probability $p_\mathcal{E}$ for that. Here, $\varnothing$ denotes the valid option that no vehicle makes a reservation for this zone at time τ. In the latter case, the remaining probability of the parent node is assigned to the corresponding edge. When the end of the prediction horizon is reached, edges are concluded with a leaf node $\mathcal{N} = \langle \varnothing, t + T_\mathrm{hor} \rangle$. A scenario consists of all edges leading from the root to the leaf node. The absolute probability of a scenario is therefore calculated as the product of all edge probabilities in this scenario:

$$p(\mathcal{S}) = \prod_{\langle V, p_\mathcal{E} \rangle \in \mathcal{S}} p_\mathcal{E}. \tag{4}$$

4) Decision Tree Exploration: As discussed in Section II-B.3, finding a potentially suboptimal solution in real-time is favored over optimality. For this, we propose the following procedure, in which we restrict the maximum number of predicted scenarios, while the prediction module aims to cover the most probable outcomes. The scenarios are explored in a greedy depth-first search by choosing the most probable unexplored edge at each node until the horizon end, i.e., a tree leaf, is reached. The root node is constructed from the first decision that is found by the prediction module. For all but the first scenario, the prediction starts at the unexplored edge with the highest absolute probability. The calculation results up to this decision can be reused to save computation time. For the evaluation in Section III-B, a maximum number of 20 predicted scenarios was chosen. With the exploration scheme above, over $95\,\%$ of the explored decisions covered more than $99\,\%$ scenario probability.

After reaching the maximum number of predicted scenarios, a concluding leaf node is attached to all remaining unexplored edges. The efficiency of unexplored scenarios is set to the lowest known efficiency e_min in the tree, as a lower bound estimation and to favor avoiding these unknown cases.

E. Maneuver Selection

The expected value of the scenario efficiency can be calculated as the average over all scenario efficiencies weighted by the scenario probability:

$$\mathrm{E}[e] = \sum_{\mathcal{S}_i} e(\mathcal{S}_i) p(\mathcal{S}_i). \tag{5}$$

The aim of the planning system is to maximize the expected efficiency. However, maneuvers should only be performed if they lead to a significant efficiency gain, as the effort to coordinate and perform a maneuver should not be neglected, which is discussed in the following.

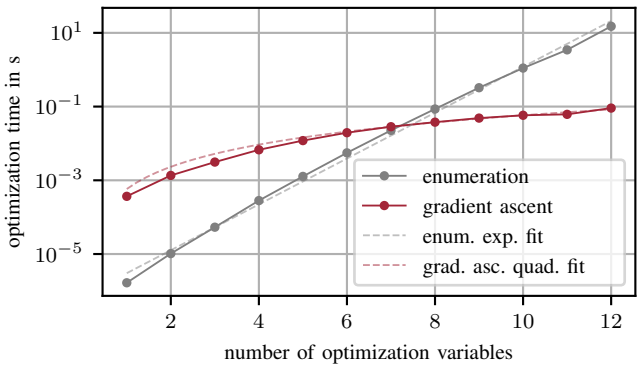

Fig. 5. Average computation time for finding the optimal maneuver using the enumeration and gradient ascent algorithms depending on the number of cooperative vehicle pairs, and respective exponential and quadratic fits.

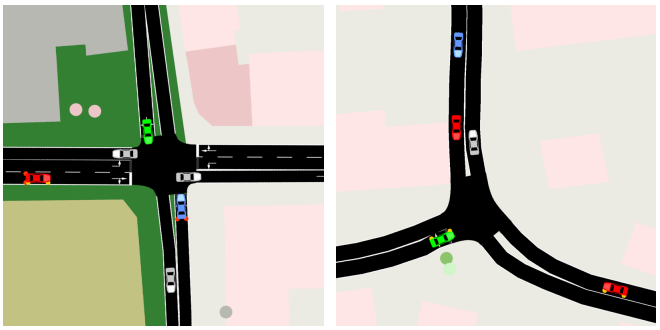

Fig. 6. Unsignalized intersections used for evaluation in SUMO [20]. Left scene (Bendplatz, Aachen): horizontal main road with separate left turn lanes. Right scene (Loherstraße, Ulm-Lehr): bending main road and side road from the left. Gray vehicles are not cooperative, blue ones are cooperative but not in a maneuver. Red vehicles yield to the prioritized green one to lower the average crossing duration.

1) Maneuver Encoding: With a maneuver coordination scheme as described in Section II-B.1, the priority between cooperative vehicles can dynamically be assigned to enforce a different crossing order. As a result, the precedence probability between a pair of cooperative vehicles can be manually set to 0 or 1 instead of leaving the decision to the drivers. This applies to each pair of cooperative vehicles that approach the same conflict zone, where N_P denotes the number of such pairs in the current planning cycle. These degrees of freedom of the planning algorithm are represented by the variables $\alpha_l \in \{-1, 0, 1\}$ ($l \in \{1, \dots, N_\mathrm{P}\}$), reflecting the influence on the precedence probability $p_{\mathcal{S},\mathrm{Z}}(i, j, \tau)$ of the l-th cooperative pair $\mathrm{V}_i, \mathrm{V}_j$ accordingly:

$$\tilde{p}_{\mathcal{S},\mathrm{Z}}(i, j, \tau) = f(p_{\mathcal{S},\mathrm{Z}}(i, j, \tau), \alpha_l) \tag{6a}$$

$$\text{with } f(p, \alpha) = \begin{cases} 0, & \text{for } \alpha = -1 \\ p, & \text{for } \alpha = 0 \\ 1, & \text{for } \alpha = 1. \end{cases} \tag{6b}$$

Each occurrence of the precedence probability between V_i and V_j in every branch of the decision tree is affected by this intervention, making the expected efficiency $\mathrm{E}[e]$ a function of the variables $\boldsymbol{\alpha} = (\alpha_1, \dots, \alpha_{N_\mathrm{P}})^\top$.

2) Optimization Objective: To take the maneuver coordination effort into account, a weighted regularizing cost term $\|\boldsymbol{\alpha}\|$ is subtracted from the expected efficiency. The problem of finding the optimal maneuver $\boldsymbol{\alpha}^*$ can now be formulated:

$$\boldsymbol{\alpha}^* = \arg\max_{\boldsymbol{\alpha}} l(\boldsymbol{\alpha}) \tag{7a}$$

$$\text{with } l(\boldsymbol{\alpha}) = \mathrm{E}[e](\boldsymbol{\alpha}) - w_\alpha \|\boldsymbol{\alpha}\|, \tag{7b}$$

where $l(\boldsymbol{\alpha})$ is the objective function. The weight w_α was empirically chosen to 1 s.

3) Enumeration: With three possibilities for each of N_P cooperative vehicle pairs, there are 3^{N_P} combinations to explore. For $N_\mathrm{P} \leq 7$, all combinations are evaluated and the most efficient maneuver is selected to be coordinated. However, for a higher number of cooperative pairs, exponentially many combinations cannot be enumerated in real-time.

4) Gradient-based optimization: We cope with the combinatorial complexity by resorting to a continuous method of optimization. $f(p, \alpha)$ is replaced by $f_\mathrm{cont}(p, \alpha)$, defined as a piecewise linear function fulfilling the constraints in Eq. (6b):

$$f_\mathrm{cont}(p, \alpha) := \begin{cases} p + \alpha p, & \text{for } \alpha < 0 \\ p, & \text{for } \alpha = 0 \\ p + \alpha(1 - p), & \text{for } \alpha > 0. \end{cases} \tag{8}$$

To optimize the objective function from Eq. (7), the gradient of $l(\boldsymbol{\alpha})$ has to be known, which depends on the gradient of f_cont along $\boldsymbol{\alpha}$. The derivates of $f_\mathrm{cont}(p, \alpha)$ are calculated as

$$\left.\frac{\partial f_\mathrm{cont}}{\partial \alpha}\right|_{p,\alpha} = \begin{cases} p, & \text{for } \alpha < 0 \\ 0.5, & \text{for } \alpha = 0 \\ 1 - p, & \text{for } \alpha > 0. \end{cases} \tag{9}$$

The best expected efficiency can now be found by performing a gradient ascent optimization of $l(\boldsymbol{\alpha})$ on $\boldsymbol{\alpha} \in [-1, 1]^{N_\mathrm{P}}$. This has a more efficient quadratic running time compared to the exponential complexity of enumeration, as shown in Fig. 5 for observed values of N_P. The problem is not convex in general and the method can find a local maximum, i.e., optimality is traded in favor of real-time capability as discussed in II-B.3. To increase chances of finding the global maximum, the optimization is run 20 times using different random starting points, with 10 gradient steps each. The average rate of finding the global maximum is thereby raised from 77 % to 91 %. After finding a solution $\boldsymbol{\alpha}^*$, its elements are rounded to the nearest integer to obtain discrete decisions.

III. Experiments

The proposed scenario prediction and maneuver selection modules were attached to and evaluated with the microscopic traffic simulation framework SUMO [20]. Two real unsignalized intersection layouts were selected for evaluation and imported from OpenStreetMap data, see Fig. 6. The first is at the Bendplatz in Aachen, Germany, consisting of a main road with separate left turn lanes and a crossing side road. A real traffic observation dataset is available for this

intersection [21]. The second scene in Ulm-Lehr, Germany, is a bending main road (Loherstraße) and a single side road, resulting in a T-junction. An example video of the simulated scenarios is available as supplementary material and at `https://youtu.be/8TUKvJsV_vA`.

A. Simulation Setup

The SUMO simulation framework was modified to support the dynamic assignment of priorities between cooperative vehicle pairs. The simulation step length and action step length were set to $0.1\,\mathrm{s}$ to allow for a microscopic reactive behavior. The *impatience* driver parameter was set to $30\,\%$ to get a realistic, not overcautious driver behavior. Beyond that, no modifications were made to keep the simulation representative. The planning modules are implemented as efficient C++ libraries embedded in a Python program, considering the real-time constraints elaborated in Section II-B.3. The software runs concurrently to the simulation to consider computational latency. Only vehicles closer than $60\,\mathrm{m}$ and farther than $10\,\mathrm{m}$ to the intersection are considered for maneuvers, to represent the limited infrastructure perception and limited reaction time, respectively. After each planning cycle, the vehicle priorities are directly sent to SUMO and handled by its modified intersection handling. The velocity of both cooperative and legacy vehicles is controlled by the driver model of the simulation framework. The default behavior of vehicles at unsignalized intersections in SUMO serves as a baseline when no cooperative vehicle is present.

The dataset [21] for the intersection in Aachen was analyzed for typical traffic density from each direction. The recordings in the dataset have a total of about 800 vehicles appearing per hour, with a high ratio of traffic on the main road. For the evaluation, varying traffic densities around this value were examined. Approaching vehicles were spawned using a reproducible random number generator at a distance of about $150\,\mathrm{m}$ to the intersection with a route distribution similar to that of the real traffic dataset. For the intersection in Ulm-Lehr, the same traffic densities are examined and, as for the other intersection, most of the vehicles are spawned on the two main road lanes.

B. Evaluation Results

The time loss due to interaction $L(\mathrm{V}_i)$ of a vehicle V_i was chosen as a quantitative evaluation measure. It is defined as

$$L(\mathrm{V}_i) \coloneqq \int_{T_\text{start}}^{T_\text{end}} 1 - \frac{v_i(t)}{v_\text{max}(\boldsymbol{x}_i(t))}\,\mathrm{d}t. \tag{10}$$

It is closely related to the efficiency term from Eq. (3), but in a more normalized way: The absolute time needed to cross the intersection does not affect this term, and for a large enough evaluation period $t \in [T_\text{start}, T_\text{end}]$, the interval length becomes irrelevant, as the interaction happens only at the intersection. Also, the time loss is comparable to other types of interaction points like construction sites, with an ideal value of $L(\mathrm{V}) = 0$ meaning no interaction at all.

Figure 7 shows the time loss averaged over 1000 simulated vehicles approaching the two considered intersections.

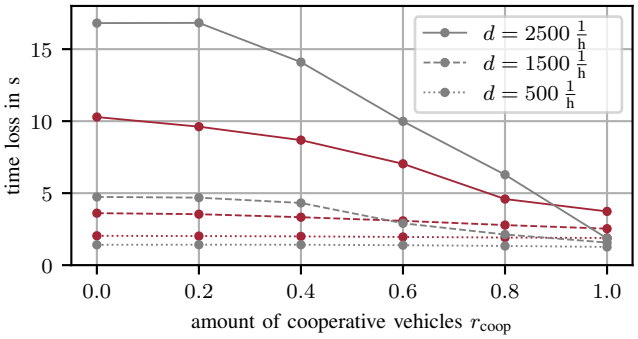

Fig. 7. Average time loss $L(\mathrm{V})$ at the intersections in Aachen (red) and Ulm-Lehr (gray). 1000 approaching vehicles were spawned randomly with varying traffic density d and increasing cooperative vehicle ratio r_coop.

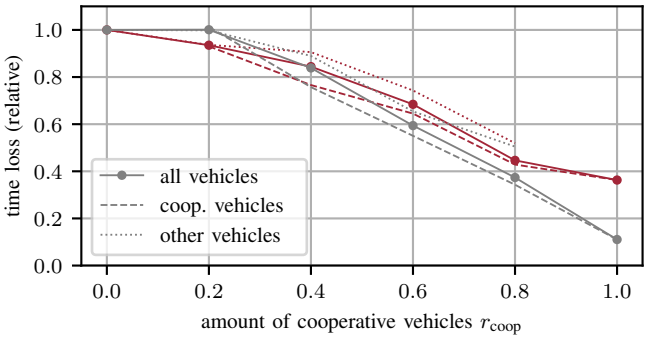

Fig. 8. Relative effect of cooperative maneuvers on the average time loss $L(\mathrm{V})$ at the intersections in Aachen (red) and Ulm-Lehr (gray), with 1000 random vehicles at a traffic density of $d = 2500\,\frac{1}{\mathrm{h}}$ and increasing cooperative vehicle ratio r_coop.

In the simulations, the cooperative vehicle rate r_coop was varied between $0\,\%$ and $100\,\%$ to show the impact of our work. The target traffic density was varied between 500 and 2500 vehicles per hour. For 1000 spawned vehicles, this corresponds to a simulation time of about 30 to $120\,\mathrm{min}$. Maneuvers can only be coordinated between two or more cooperative vehicles that approach the same conflict zone at the same time. Whenever legacy vehicles are present, as in [12], they are assumed to take the most conflicting route and may prevent maneuver planning. Therefore, with a low cooperative vehicle deployment rate, only few maneuvers can be planned. However, starting at a ratio of about $r_\text{coop} = 40\,\%$ cooperative vehicles, a significant efficiency improvement can be observed. The average time loss at the intersection in Aachen is lower due to the higher number of available lanes.

In Fig. 8, the relative impact of cooperative maneuvers on the time loss at a traffic density of $d = 2500\,\frac{1}{\mathrm{h}}$ is shown. While legacy vehicles can only benefit from an increased traffic flow, cooperative vehicles directly have a lower time loss with each performed maneuver, so there is a higher impact even at a low cooperative vehicle ratio. At the intersection in Aachen, at $r_\text{coop} = 20\,\%$, the time loss of cooperative vehicles is already reduced by $7.0\,\%$. In Ulm-Lehr, the intersection can be blocked by legacy vehicles

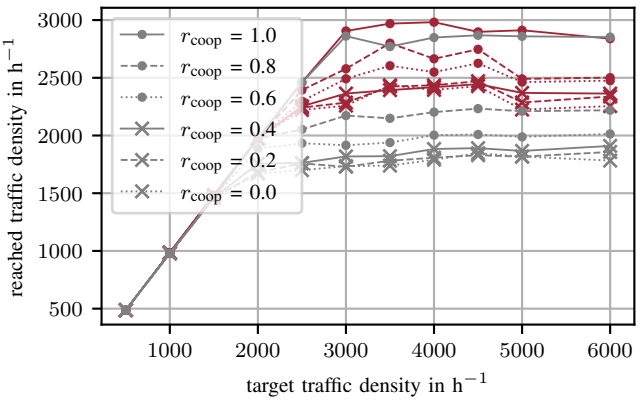

Fig. 9. Reachable traffic throughput at the intersections in Aachen (red) and Ulm-Lehr (gray), averaged over 1000 random vehicles, with varying cooperative vehicle ratio r_{coop} and an increasing target traffic density.

more easily and a significant reduction of the time loss of $24.3\,\%$ can be observed at $r_{\text{coop}} = 40\,\%$ (Aachen: reduced by $23.4\,\%$). The time loss of single vehicles is increased in some cases, which can also affect legacy vehicles if they are behind a cooperative vehicle yielding to another. However, the time loss averaged over the vehicles in a particular scenario is not increased by the performed maneuvers, and legacy vehicles are not disadvantaged by the cooperation of others.

Figure 9 shows the reachable traffic throughput at the two intersections at varying cooperative vehicle ratios. The target traffic density, i.e., spawn rate, is incrementally increased, however the spawning of vehicles is delayed if too many vehicles accumulate at the intersection and block the spawning point. With an increasing amount of cooperative vehicles, a traffic flow of up to $26\,\%$ (Aachen) and $60\,\%$ (Ulm-Lehr) higher than without cooperative vehicles is achievable.

The evaluation shows that already at a low cooperative vehicle ratio, an increase in traffic flow can be observed, depending on the intersection layout. As can be expected, the more cooperative vehicles participate, the higher are the traffic flow and efficiency gains that can be achieved.

IV. Conclusion

In this paper, we presented a new planning system to improve the traffic efficiency at unsignalized intersections by performing cooperative maneuvers between connected vehicles. We showed that our approach can computationally efficiently handle a high density of mixed traffic and different kinds of intersection layouts. Our evaluation revealed that even with a low ratio of cooperative vehicles, a noticeable efficiency and traffic flow gain can be achieved.

In future work, we will implement the system in reality at the intersection in Ulm-Lehr to prove our simulation results and study the effects of driver interaction latency. Also, we will adapt our planning approach to other scenarios, such as overtaking and a shared single lane for traffic in both directions, showing that cooperative maneuvers can achieve efficiency gains in various situations.

References

[1] ETSI TR 103 578, "Intelligent Transport Systems (ITS); Vehicular Communication; Informative Report for the Maneuver Coordination Service," 2020, draft V0.0.5.

[2] K. Dresner and P. Stone, "Sharing the Road: Autonomous Vehicles meet Human Drivers," in *The 20th Int. Joint Conf. on Artificial Intelligence*, 2007, pp. 1263–68.

[3] X.-H. Yu and A. Stubberud, "Markovian decision control for traffic signal systems," in *Proc. of the 36th IEEE Conf. on Decision and Control*, vol. 5, 1997, pp. 4782–4787 vol.5.

[4] J. Wu, A. Abbas-Turki, and A. El Moudni, "Cooperative driving: an ant colony system for autonomous intersection management," *Appl Intell*, vol. 37, no. 2, pp. 207–222, 2012.

[5] K. Dresner and P. Stone, "Multiagent traffic management: a reservation-based intersection control mechanism," in *Proc. of the Third Int. Joint Conf. on Autonomous Agents and Multiagent Syst., 2004. AAMAS 2004.*, 2004, pp. 530–537.

[6] L. Li and F.-Y. Wang, "Cooperative Driving at Blind Crossings Using Intervehicle Communication," *IEEE Transactions on Veh. Technol.*, vol. 55, no. 6, pp. 1712–1724, 2006.

[7] F. Yan, M. Dridi, and A. El Moudni, "Autonomous vehicle sequencing algorithm at isolated intersections," in *2009 12th Int. IEEE Conf. on Intell. Transp. Syst.*, 2009, pp. 1–6.

[8] R. Hult, M. Zanon, S. Gras, and P. Falcone, "An MIQP-based heuristic for Optimal Coordination of Vehicles at Intersections," in *2018 IEEE Conf. on Decision and Control (CDC)*, 2018, pp. 2783–2790.

[9] K. Yang, S. I. Guler, and M. Menendez, "Isolated intersection control for various levels of vehicle technology: Conventional, connected, and automated vehicles," *Transp. Research Part C: Emerging Technologies*, vol. 72, pp. 109–129, 2016.

[10] K. Kurzer, C. Zhou, and J. Marius Zöllner, "Decentralized Cooperative Planning for Automated Vehicles with Hierarchical Monte Carlo Tree Search," in *2018 IEEE Intell. Veh. Symp. (IV)*, 2018, pp. 529–536.

[11] M. Klimke, B. Völz, and M. Buchholz, "Cooperative Behavior Planning for Automated Driving using Graph Neural Networks," in *2022 IEEE Intelligent Vehicles Symposium (IV)*, to be published. [Online]. Available: https://arxiv.org/abs/2202.11376

[12] L. C. Bento, R. Parafita, S. Santos, and U. Nunes, "Intelligent traffic management at intersections: Legacy mode for vehicles not equipped with V2V and V2I communications," in *16th Int. IEEE Conf. on Intell. Transp. Syst. (ITSC 2013)*, 2013, pp. 726–731.

[13] F. Perronnet, A. Abbas-Turki, and A. El Moudni, "A sequenced-based protocol to manage autonomous vehicles at isolated intersections," in *16th Int. IEEE Conf. on Intell. Transp. Syst. (ITSC 2013)*, 2013, pp. 1811–1816.

[14] M. Ahmane, A. Abbas-Turki, F. Perronnet, J. Wu, A. E. Moudni, J. Buisson, and R. Zeo, "Modeling and controlling an isolated urban intersection based on cooperative vehicles," *Transp. Research Part C: Emerging Technologies*, vol. 28, pp. 44–62, 2013.

[15] M. Nichting, D. Heß, J. Schindler, T. Hesse, and F. Köster, "Space Time Reservation Procedure (STRP) for V2X-Based Maneuver Coordination of Cooperative Automated Vehicles in Diverse Conflict Scenarios," in *2020 IEEE Intell. Veh. Symp. (IV)*, 2020, pp. 502–509.

[16] M. B. Mertens, J. Müller, R. Dehler, M. Klimke, M. Maier, S. Gherekhloo, B. Völz, R.-W. Henn, and M. Buchholz, "An Extended Maneuver Coordination Protocol with Support for Urban Scenarios and Mixed Traffic," in *2021 IEEE Veh. Netw. Conf. (VNC)*, 2021, pp. 32–35.

[17] ETSI ES 202 663, "Intelligent Transport Systems (ITS); European profile standard for the physical and medium access control layer of Intelligent Transport Systems operating in the 5 GHz frequency band," 2009, final draft V1.1.0.

[18] M. Treiber, A. Hennecke, and D. Helbing, "Congested Traffic States in Empirical Observations and Microscopic Simulations," *Phys. Rev. E*, vol. 62, no. 2, pp. 1805–1824, 2000.

[19] J. Erdmann and D. Krajzewicz, "SUMO's Road Intersection Model," in *Simulation of Urban Mobility*. Springer, 2014, vol. 8594, pp. 3–17.

[20] P. A. Lopez, M. Behrisch, L. Bieker-Walz, J. Erdmann, Y.-P. Flötteröd, R. Hilbrich, L. Lücken, J. Rummel, P. Wagner, and E. Wießner, "Microscopic Traffic Simulation using SUMO," in *21st IEEE Int. Conf. on Intell. Transp. Syst.*, 2018, pp. 2575–2582.

[21] J. Bock, R. Krajewski, T. Moers, S. Runde, L. Vater, and L. Eckstein, "The inD Dataset: A Drone Dataset of Naturalistic Road User Trajectories at German Intersections," 2019. [Online]. Available: http://arxiv.org/abs/1911.07602